Gait & Posture 39 (2014) 518–522

Contents lists available at ScienceDirect

Gait & Posture

journal homepage: www.elsevier.com/locate/gaitpost

Ellipse area calculations and their applicability in posturography

Patric Schubert [1,*], Marietta Kirchner [1]

Department of Health, Fresenius University of Applied Sciences, Limburger Straße 2, 65510 Idstein, Germany

ARTICLE INFO

Article history:
Received 18 July 2012
Received in revised form 18 June 2013
Accepted 3 September 2013

Keywords:
Posturography
Postural control
COP area calculation
Prediction ellipse
Confidence ellipse

ABSTRACT

The quantification of postural sway is considered to be an essential part of posturography and is important for research and clinical utility. A widely used method to calculate the scatter of center of pressure data is an ellipse that encloses about $100(1-\alpha)\%$ of the observations. However, underlying definitions and terminologies have been misused in many cases. Hence, outcomes of different studies are proved to be incommensurable. In order to attain inter-study comparability, standardization of calculation methods has to be advanced. This work features a comprehensive and consistent overview of the methods for elliptic area approximation contrasting general principles of confidence and prediction regions. As a result, we recommend the usage of the prediction ellipse, as far as we demonstrate that confidence ellipses emerge to be inappropriate for posturographic scatter evaluation. Furthermore, we point at problems that come along with different sample sizes.

1. Introduction

If a subject is asked to stand as still as possible on a force plate, small oscillations of the center of pressure (COP) can be observed [1]. Quantification of these fluctuations is considered to be an essential part of posturography and is important for research and clinical utility [2]. Among a great variety of parameters the computation of sway area is a traditional and widely used method. A geometrically simple figure is an ellipse that encloses about $100(1-\alpha)\%$ of the observations in the scatter plot [3]. However, as an ellipse including this characteristic cannot be univocally constructed, terminologies have to be formulated more precisely. However, with respect to literature, definitions and terminologies have been misused in many cases. For instance, Prieto et al. [4] and Prieto and Myklebust [5] use the term 'confidence ellipse'; however, underlying calculations are conceptually referred to 'prediction ellipses' which was spuriously adopted by several authors [6–10]. Both terms are the bivariate analogs of the univariate views on confidence and prediction intervals with different prerequisites and underlying formulas. Moreover, some confusion prevails concerning calculation methods. As in the past computations implemented regression analysis, more recent investigations are based on the theories of principal component analysis (PCA) in order to gain uniqueness of the ellipse. The latter method is proposed by Oliveira et al. [11] which to their point of view "does not appear to have been considered for this purpose before". First, the introduced procedure can be reduced to an Eigen value problem. Second, similar procedures have been published by others yet [5,12].

The quite simple formulas and procedures were unnecessarily complicated by many authors and it can be shown that they could be merged into each other. In addition, some formal mistakes regarding published equations [4,7,13] are revealed. Inter-study comparisons in posturography require adequate standardization of the calculation methods. This work features a comprehensive and consistent overview of the methods for elliptic area approximation contrasting the principles of confidence and prediction ellipses.

2. Basic considerations

For this purpose, we have to differentiate between the construction of confidence and prediction regions. Therefore, we present basic assumptions from a statistical point of view. Subsequently, we refer specifically to area calculation of confidence and prediction ellipses.

2.1. Confidence and prediction intervals

First, we would like to reduce the distinction to the univariate case [14]. In practice, the population mean μ and its standard deviation σ are not known. One estimates the true population mean μ from the observed data and asks how good the estimation is. When $\bar{x}$ is the sample mean, one would like to define a region around $\bar{x}$ which covers with $100(1-\alpha)\%$ of probability the true value μ. Let $\bar{X} = 1/n \sum_{i=1}^{n} X_i$ be the estimation function. According

* Corresponding author. Tel.: +49 6126 935 2293.
E-mail addresses: rough@ironsport.de, Patric.schubert@hs-fresenius.de, p.schubert@sport.uni-frankfurt.de (P. Schubert).
[1] Both authors contributed equally to this paper.

0966-6362/$ – see front matter © 2013 Elsevier B.V. All rights reserved.
http://dx.doi.org/10.1016/j.gaitpost.2013.09.001

to the central limit theorem $\bar{X}$ follows a normal distribution. That is, $\bar{X} \sim N(\mu, \sigma^2/n)$ which results in $(\bar{X}-\mu) \sim N(0, \sigma^2/n)$. Denote a random variable $Z_C = \bar{X} - \mu$ with mean 0 and standard deviation $\sigma/\sqrt{n}$. Then we can define

$$P\left(-z_{(1-\alpha/2)} \leq \frac{Z_C}{\sigma/\sqrt{n}} \leq z_{(1-\alpha/2)}\right) = 1-\alpha, \quad (1)$$

with $z_{(1-\alpha/2)}$ being the $(1-\alpha/2)$-quantile of the standard normal distribution. This can be transformed into

$$P\left(\bar{X} - z_{(1-\alpha/2)}\frac{\sigma}{\sqrt{n}} \leq \mu \leq \bar{X} + z_{(1-\alpha/2)}\frac{\sigma}{\sqrt{n}}\right) = 1-\alpha. \quad (2)$$

With respect to a realization based on a sample of size n where the unknown standard deviation σ is estimated by $s = \sqrt{(1/(n-1))\sum_{i=1}^{n}(x_i-\bar{x})^2}$ the confidence interval is given by [14]

$$\left[\bar{x} - t_{(1-\alpha/2),n-1}\frac{s}{\sqrt{n}}; \bar{x} + t_{(1-\alpha/2),n-1}\frac{s}{\sqrt{n}}\right], \quad (3)$$

with $t_{(1-\alpha/2),n-1}$ being the $(1-\alpha/2)$-quantil of the t-distribution with $(n-1)$ degrees of freedom. The t-distribution converges against the normal distribution for large n. The confidence interval determines a region which covers with $100(1-\alpha)$% of probability the unknown population mean.

In contrast, prediction intervals estimate an unknown future observation from the statistic of the observed sample. The task is to create limits to the sample mean $\bar{x}$ so that with $100(1-\alpha)$% of probability the future observation will fall into the prediction interval. Let Z be a new single observation. We define a random variable $Z_P = Z - \bar{X}$ with mean 0 and standard deviation $\sigma \cdot \sqrt{1+(1/n)}$. As before (Eq. (1)) we have

$$P\left(-z_{(1-\alpha/2)} \leq \frac{Z_P}{\sigma \cdot \sqrt{1+(1/n)}} \leq z_{(1-\alpha/2)}\right) = 1-\alpha, \quad (4)$$

which gives a prediction interval [14]

$$\left[\bar{x} - t_{(1-\alpha/2),n-1}s\sqrt{1+\frac{1}{n}}; \bar{x} + t_{(1-\alpha/2),n-1}s\sqrt{1+\frac{1}{n}}\right]. \quad (5)$$

Confidence intervals will shrink as the sample size n increases because $\lim_{n\to\infty} 1/\sqrt{n} = 0$. Prediction intervals, on the other hand, will have a limit of $(z_{(1-\alpha/2)} \cdot s)$ as it is $\lim_{n\to\infty} t_{(1-\alpha/2),n-1} = z_{(1-\alpha/2)}$ and $\lim_{n\to\infty}\sqrt{1+(1/n)} = 1$. In opposition to confidence intervals, they have to cope with both the uncertainty of the true population mean and the scatter of the sample, which means that the region is on average broader.

2.2. Confidence and prediction ellipses

The theories on confidence and prediction regions can be extended to the multivariate case. In posturography a bivariate view complies with this purpose (see Appendix section c). For large n, the bivariate confidence region is a confidence ellipse, which can be seen as the contour lines of the bell-shaped mound of the bivariate normal population distribution. Two parameters are required (we denote vectors and matrices in bold letters): the population mean vector $\mu = \begin{pmatrix}\mu_x \\ \mu_y\end{pmatrix}$ for which the estimate function is $\bar{X} = \frac{1}{n}\begin{pmatrix}\sum_{i=1}^{n} X_i \\ \sum_{i=1}^{n} Y_i\end{pmatrix}$, and population covariance matrix $\Sigma = \begin{pmatrix}\sigma_x^2 & \sigma_{x,y} \\ \sigma_{x,y} & \sigma_y^2\end{pmatrix}$, which is estimated by the unbiased sample covariance matrix $S = \begin{pmatrix}s_x^2 & s_{x,y} \\ s_{x,y} & s_y^2\end{pmatrix}$. The random variable $Z_C = \bar{X} - \mu$ then has mean 0 and covariance $(1/n)\,\Sigma$ (estimated by $(1/n)\,S$). We can write (see Appendix section a):

$$P\left(n \cdot {Z_C}^T S^{-1} Z_C \leq T^2_{(1-\alpha),2,n-2}\right) = 1-\alpha \quad (6)$$

where $(\cdot)^T$ is the transpose and T^2 is the Hotelling T-squared distribution with 2 and $(n-2)$ degrees of freedom which forms the multivariate generalization of the t-distribution [15]. It can be shown that $T^2_{2,n-2} = (2(n-1)/(n-2))\,F_{2,n-2}$, where $F_{2,n-2}$ is the Fisher-distribution with 2 and $(n-2)$ degrees of freedom [16]. A similar notation to Eq. (6) can be found in Sokal and Rohlf [3]. We expect the confidence ellipse covers with a $100(1-\alpha)$% of probability the true population mean μ.

With respect to posturography, we want to describe the ellipse itself. The directions x and y are now referred to the medial–lateral and the anterior–posterior component of the COP motion with sample mean $\bar{x} = \begin{pmatrix}\bar{x} \\ \bar{y}\end{pmatrix}$. After the division by n we get

$$(\bar{x}-\mu)^T S^{-1}(\bar{x}-\mu) = \frac{2(n-1)}{n(n-2)}F_{(1-\alpha),2,n-2}. \quad (7)$$

The left side can be also merged into

$$\frac{s_x^2 s_y^2}{s_x^2 s_y^2 - s_{xy}^2}\left[\frac{(\bar{x}-\mu_x)^2}{s_x^2} + \frac{(\bar{y}-\mu_y)^2}{s_y^2} - \frac{2s_{xy}(\bar{x}-\mu_x)(\bar{y}-\mu_y)}{s_x^2 s_y^2}\right] = \frac{2(n-1)}{n(n-2)}F_{(1-\alpha),2,n-2}. \quad (8)$$

This equation can now be solved to get a region around μ_x and μ_y with a given probability of $100(1-\alpha)$% as this is preset by the F-value.

An equal form can be looked-up in Rocchi et al. [17]. However, the authors mix the theories of confidence and prediction ellipses as they talk of confidence but calculate prediction ellipses. The right side of Eq. (8) demonstrates a coefficient which limits the size of the confidence ellipse. With larger n its size will shrink: $\lim_{n\to\infty} 2(n-1)/n(n-2) = 0$ (for $n > 101$ the coefficient is less than 0.01). If the experimenter wants to describe the scatter or covariation of the data, a prediction ellipse will be more appropriate. Consider $\mathbf{Z}$ as a vector of a new observation and $\boldsymbol{Z_P} = \boldsymbol{Z} - \bar{\boldsymbol{X}}$ a random variable with mean 0 and covariance $(1+1/n)\boldsymbol{\Sigma}$. Then, the probability of the prediction region can be denoted as

$$P\left(\left(1+\frac{1}{n}\right)^{-1} \cdot {Z_P}^T S^{-1} Z_P \leq T^2_{(1-\alpha),2,n-2}\right) = 1-\alpha. \quad (9)$$

Multiplying the factor $(n+1)/n$ the equation for the prediction ellipse is then defined by [18]:

$$(z-\bar{x})^T S^{-1}(z-\bar{x}) = \frac{2(n+1)(n-1)}{n(n-2)}F_{(1-\alpha),2,n-2}. \quad (10)$$

For large n it is $\lim_{n\to\infty} 2(n+1)(n-1)/n(n-2)F_{(1-\alpha),2,n-2} = 2F_{(1-\alpha),2,n-2}$ (for $n > 202$ the coefficient is less than 1.01). The right side approaches the Chi square distribution with 2 degrees of freedom: $\lim_{n\to\infty} 2 \cdot F_{(1-\alpha),2,n-2} \sim \chi^2_{(1-\alpha),2}$. The bivariate prediction region is an ellipse that covers with $100(1-\alpha)$% of probability the future observation $\mathbf{Z}$. A $100(1-\alpha)$% prediction region for the next observation is identical to a $100(1-\alpha)$% tolerance region of type 2, due to the following definition: A bivariate tolerance region is an ellipse such that the expected value of the proportion of the population contained in the ellipse is exactly $100(1-\alpha)$% [18].

The constructions of confidence and prediction regions differ in their assumptions. Both regions are located around the sample

mean; however, they describe different aspects of the sample. As we have separated the theories of confidence and prediction regions we now turn toward the main issue: the area calculation of confidence and prediction ellipses.

2.3. Area calculation

It is known from analytical geometry that the area A_E of an ellipse is defined as the product of the principal axes with pi:

$$A_E = \pi ab \tag{11}$$

The prime task is henceforth to get the principal axes of the ellipse. There are two possibilities to define the major axis of the ellipse. By means of regression analysis one can find an axis that passes through the point $(\bar{x}, \bar{y})$ so that the deviation of observed values from regression is minimal [3]. However, deviations are defined parallel to the abscissa, which gives two different solutions: x is drawn versus y or vice versa, as demonstrated by e.g., Oliveira et al. [11]. So, another criterion should be that deviations are at right angles to the major axis itself and are at minimum. This will lead to an Eigen value problem which involves the determination of the Eigen values λ_1 and λ_2 from the sample covariance matrix, $|\mathbf{S} - \lambda\mathbf{E}| = 0$ where $\mathbf{E}$ stands for the unity matrix. We solve the Eigen values by

$$\lambda_{1/2} = \frac{1}{2}\left[s_x^2 + s_y^2 \pm \sqrt{\left(s_x^2 - s_y^2\right)^2 + 4s_{xy}^2}\right]. \tag{12}$$

A part of the computation of the axes of the confidence ellipse is equal to the one of the prediction ellipse. The semimajor and semiminor axes of the confidence ellipse are

$$a_C = \sqrt{\frac{2(n-1)}{n(n-2)}F_{(1-\alpha),2,n-2}\cdot\lambda_1} \approx \sqrt{\chi_2^2\cdot\frac{\lambda_1}{n}} \tag{13}$$

$$b_C = \sqrt{\frac{2(n-1)}{n(n-2)}F_{(1-\alpha),2,n-2}\cdot\lambda_2} \approx \sqrt{\chi_2^2\cdot\frac{\lambda_2}{n}} \tag{14}$$

and with Eq. (11) the confidence ellipse area (CEA) can be resolved to

$$\begin{aligned}\mathrm{CEA} &= \pi a_C b_C = \pi\frac{2(n-1)}{n(n-2)}F_{(1-\alpha),2,n-2}\cdot\sqrt{\lambda_1\lambda_2} \\ &\approx \pi\frac{1}{n}\chi_2^2\cdot\sqrt{\lambda_1\lambda_2} = \pi\frac{1}{n}\chi_2^2\sqrt{\det(\mathrm{S})}.\end{aligned} \tag{15}$$

The semimajor and semiminor axes of the prediction ellipse are

$$a_P = \sqrt{\frac{2(n+1)(n-1)}{n(n-2)}F_{(1-\alpha),2,n-2}\cdot\lambda_1} \approx \sqrt{\chi_2^2\cdot\lambda_1} \tag{16}$$

$$b_P = \sqrt{\frac{2(n+1)(n-1)}{n(n-2)}F_{(1-\alpha),2,n-2}\cdot\lambda_2} \approx \sqrt{\chi_2^2\cdot\lambda_2}. \tag{17}$$

The area of the prediction ellipse (PEA) is then

$$\begin{aligned}\mathrm{PEA} &= \pi a_P b_P = \pi\frac{2(n+1)(n-1)}{n(n-2)}F_{(1-\alpha),2,n-2}\cdot\sqrt{\lambda_1\lambda_2} \\ &\approx \pi\chi_2^2\cdot\sqrt{\lambda_1\lambda_2} = \pi\chi_2^2\sqrt{\det(\mathrm{S})}.\end{aligned} \tag{18}$$

The formulas of CEA and PEA differ merely in the coefficient $1/n$, however this is an important fact considering the outcome. We have illustrated both ellipses in Fig. 1. We further point to the equivalence in outcome of PEA and the method of PCA calculation for large n. As in PCA the confidence interval is calculated as an interval of dispersion of the sample, the standard deviation σ is used instead of $\sigma\cdot\sqrt{1+(1/n)}$ (compare Eq. (4) for univariate case and Eq. (9) for bivariate case). This leads to identical assumptions of the PCA method compared to PEA as shown by the paragraph after Eq. (10).

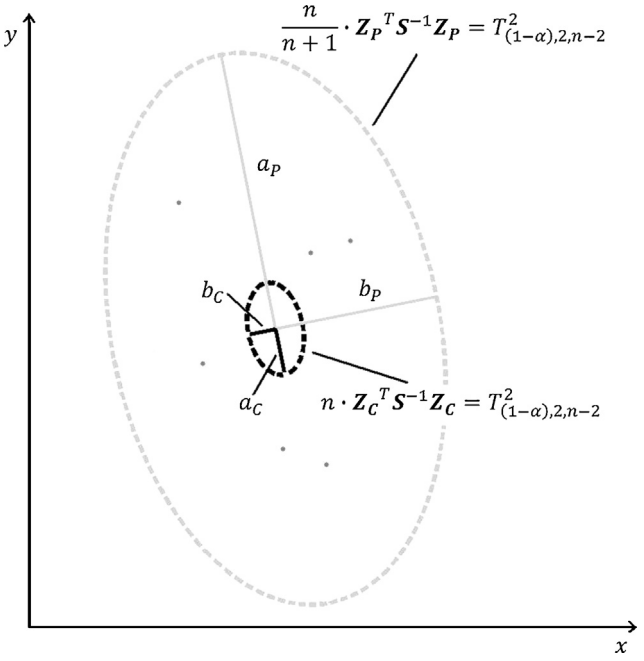

Fig. 1. Prediction ellipse (gray) and confidence ellipse (black) of the same sample ($n = 6$). The confidence ellipse covers with a certain probability the population mean. In contrast, the prediction ellipse covers with the same probability a future observation. Thus, the area of the confidence ellipse (CEA) is on average smaller than the area of the prediction ellipse (PEA). (a_P,b_P prediction ellipse semi axes; a_c,b_c confidence ellipse semi axes.)

3. Results

Concerning CEA, we see that increasing the sample size by a factor k the area is shrinking by approximately k^2. This is an immediate result of Eq. (15) (which reduces the size formally by k) and of the typical unimodal characteristic of the COP that has influence on the standard deviations and hence, on Eq. (12). In opposition, downsampling has a negligible effect on the extent of

Table 1
List of symbols and notations.

Symbol	Declaration
α	Probability value between $[0, 1]$
μ	Population mean
σ^2	Population variance
n	Sample size
X_i	ith random variable of the sample
$\bar{X} = \frac{1}{n}\sum_{i=1}^{n} X_i$	Estimation function of the sample mean
$\frac{s}{\sqrt{n}}$	Standard error
$s = \frac{1}{n-1}\sum_{i=1}^{n}(x_i - \bar{x})^2$	Sample variance
μ_x, μ_y	Population means of x and y
σ_x^2, σ_y^2	Population variances in x and y direction
$\sigma_{x,y}$	Population covariance between x and y
$\bar{x}, \bar{y}$	Sample means of x and y
$s_x^2 = \frac{1}{n-1}\sum_{i=1}^{n}(x - \bar{x})^2$	Sample variance in x direction
$s_y^2 = \frac{1}{n-1}\sum_{i=1}^{n}(y - \bar{y})^2$	Sample variance in y direction
$s_{x,y} = \frac{1}{n-1}\sum_{i=1}^{n}(x - \bar{x})(y - \bar{y})$	Sample covariance between x and y
$\det(\cdot)$	Determinant function
$P(\cdot)$	Probability function

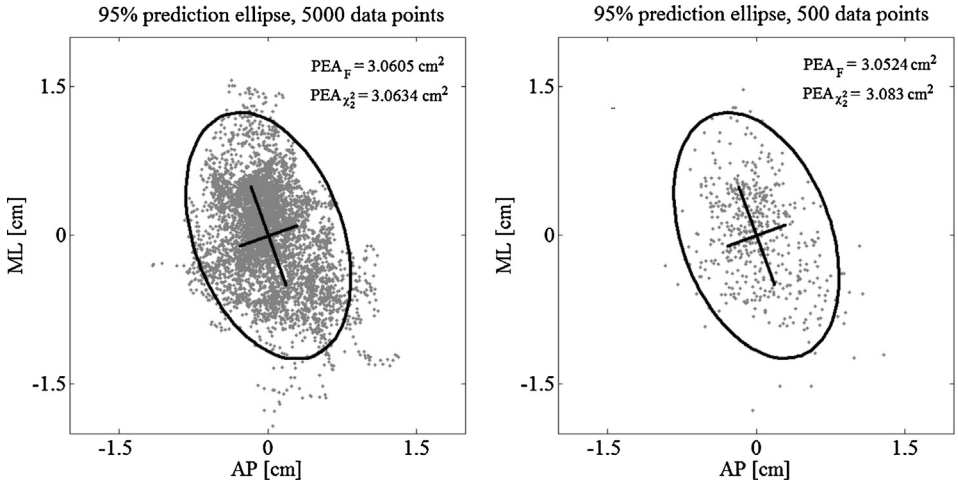

Fig. 2. Prediction ellipse calculations based on the Chi squared value concerning different sample sizes (left: 5000 data points, right: 500 data points; downsampled by factor 10). The black cross inside the ellipses indicates the direction of the major and minor axes (the length is normalized to the Eigen values of the sample points). Prediction ellipse areas are indicated with respect to the Chi-squared value (PEA χ_2^2) and to the *F*-value (PEA_F) showing a marginal difference between both calculation methods.

PEA for sufficiently large *n* (Fig. 2). The error between the *F*-value formula and the corresponding χ_2^2 value formula in Eq. (18) for PEA at $p = 95\%$ is ≈1% for $n = 500$, ≈0.5% for $n = 1000$, and ≈0.1% for $n = 5000$ (Fig. 2).

Given a set of COP data, the value of PEA can be obtained from the following algorithm (a Matlab® implementation to calculate and to plot PEA can be found in the Appendix section d and e):

Step 1: Calculate the sample variance in *x* and *y* direction and the sample covariance between *x* and *y* (Table 1).

Step 2: Calculate both Eigen values of the sample variance covariance matrix (Eq. (12)).

Step 3: Look up the value of the inverse of the chi-square cumulative distribution function with 2 degrees of freedom at a fixed probability level (usually $P = 95\%$, $\chi^2_{0.95,2} \approx 5.99146$).

Step 4: To obtain PEA, take the square root of the product of both Eigen values and multiply with pi and the value of step 3.

4. Discussion

Prediction and confidence ellipses diverge with respect to formal assumptions. On account of these discrepancies and with regard to the utility in posturography, the term 'confidence ellipse' has been misused in various publications. Authors used the concept of 'prediction ellipse' to evaluate the magnitude of COP variability or mixed both approaches. Thus, correct terminologies have to be preserved. Confidence ellipses emerge to be inappropriate for COP scatter evaluation. Increasing *n* evidently, affords a better estimator covering the true population mean. As confidence ellipses are subject of inferential statistics, Batschelet [19] adduced the application of the standard ellipse as a descriptive tool in scatter plots (which is proposed by Rocchi et al. [17] for posturographic analysis). In the standard ellipse the statistical value is set to unity, thus $\chi_2^2 = 1$. However, this is just a special case of the prediction ellipse for which the area covers with approximately 63.1% of prediction the future value **Z** (which can be appreciated by use of an inverse calculation for $n > 200$). Other authors propose different statistical scaling coefficients. Duarte and Zatsiorsky [20] and Oliveira et al. [11] use 1.96, which is the 97.5 percentile of the normal distribution. The authors claim that the resulting ellipse will contain 85.35% of the data. This is misworded as it has to be formulated that the ellipse is covering with 85.35% of probability a future data point. Moreover, the value is only exact in a range of 87–110 sample points. For $n > 200$ it is 85.60% and approaches 85.91% for large n. We point to further mistakes concerning the value 1.96. Mochizuki et al. [21] relate it to 83.35%, and Doumas et al. [22] indicate 88%. With regard to ellipse axes scaling, Chiari et al. [8] cite literature based on deviating values, for which area calculation is not evident at all. In terms of standardization and comparisons between different studies, a uniform procedure has to be advanced. If the *F*-value is applied an indication of the sample size *n* will be necessary due to the degrees of freedom (DOF). The Chi squared value χ_2^2 (two DOFs) is more practical as it forms a constant independent of the sample size *n*. Duarte et al. [23,24] suggest the value 2.4478 which is the square root of $\chi^2_{0.95,2}$. As it is shown, the error between the areas obtained from the *F*-value and the Chi squared value at $p = 95\%$ is negligible with regard to a sufficiently large sample size.

Concerning posturographic measurements, the number of samples can be increased by means of two procedures. First, it is possible to take a longer measurement duration, which will naturally lead to more data points. Under physiological aspects, one gets information within a longer time scale range regarding the postural control process. Thus, even low frequencies could be detected which is important for the assessment of the temporal organization of the COP motion [25]. Second, the data points could be increased by raising the sampling rate. However, it is evident that 95% of sway energy comprises frequencies below 1 Hz [25,26]. Augmentation of sample points over this limit will generate artificial high-frequency data inside the low-frequency physiological process. Hence, sampling rates have to be adjusted or downsampled. As 10 Hz is assumed to be an adequate cutoff value for a low-pass filter in posturography [27,28], we recommend subsequent to the filtering, a downsampling of 20 Hz prior to the analysis.

Appendix A. Supplementary data

Supplementary data associated with this article can be found, in the online version, at http://dx.doi.org/10.1016/j.gaitpost.2013.09.001.

References

[1] Latash M. Neurophysiological basis of movement. 2nd ed. Champaign, Windsor, Leeds, Lower Mitcham, North Shore City: Human Kinetics; 2008.

[2] Visser JE, Carpenter MG, van der Kooij H, Bloem BR. The clinical utility of posturography. Clin Neurophysiol 2008;119(11):2424–36.
[3] Sokal RR, Rohlf FJ. Biometry. 3rd ed. New York: W.H. Freeman and Company; 1995.
[4] Prieto T, Myklebust J, Hoffmann R, Lovett E, Myklebust B. Mesasures of postural steadiness: differences beween healthy young and elderly adults. IEEE Trans Biomed Eng 1996;43:956–66.
[5] Prieto T, Myklebust J. Measures of postural sway – letter to editor. Clin Pharmacol Ther 1993;54:228.
[6] Jørgensen MB, Skotte JH, Holtermann A, Sjøgaard G, Petersen NC, Søgaard K. Neck pain and postural balance among workers with high postural demands – a cross-sectional study. BMC Musculoskelet Disord 2011;12:176.
[7] Cavalheiro GL, Almeida MFS, Pereira AA, Andrade AO. Study of age-related changes in postural control during quiet standing through linear discriminant analysis. Biomed Eng Online 2009;8:35.
[8] Chiari L, Rocchi L, Cappello C. Stabilometric parameters are affected by anthropometry and foot placement. Clin Biomech 2002;17(9–10):666–77.
[9] Rocchi L, Chiari L, Horak FB. Effects of deep brain stimulation and levodopa on postural sway in Parkinson's disease. J Neurol Neurosurg Psychiatry 2002;73(3):267–74.
[10] Chiari L, Bertani A, Cappello C. Classification of visual strategies in human postural control by stochastic parameters. Hum Mov Sci 2000;19(6):817–42.
[11] Oliveira LF, Simpson DM, Nadal J. Calculation of area of stabilometric signals using principal component analysis. Physiol Meas 1996;17(4):305–12.
[12] Takagi A, Fujimura E, Suehiro S. A new method of statokinesigram area measurement. Application of a statistically calculated ellipse. In: Igarashi M, Black O, editors. Vestibular and visual control on posture and locomotor equilibrium. Bâle: Karger; 1985. p. 74–9.
[13] Moghadam M, Ashayeri H, Salavati M, Sarafzadeh J, Taghipoor KD, Saeedi A, Salehi R. Reliability of center of pressure measures of postural stability in healthy older adults: effects of postural task difficulty and cognitive load. Gait Posture 2011;33(4):651–5.
[14] Proschan F. Confidence and tolerance intervals for the normal distribution. J Am Stat Assoc 1953;48(263):550–64.
[15] Hotelling H. The generalization of Student's ratio. Ann Math Stat 1931;2:360–78.
[16] Jackson JE. A users guide to principal components. New York, Chichester, Brisbane, Toronto, Singapore: John Wiley & Sons; 1991.
[17] Rocchi MBL, Sisti D, Ditroilo M, Calavalle A, Panebianco R. The misuse of the confidence ellipse in statokinesigram. J Sport Sci 2005;12(2):169–71.
[18] Chew V. Confidence, prediction and tolerance regions for the multivariate normal distribution. J Am Stat Assoc 1966;61(315):605–17.
[19] Batschelet E. Circular statistics in biology. London: Academic Press; 1981.
[20] Duarte M, Zatsiorsky VM. Effects of body lean and visual information on the equilibrium maintenance during stance. Exp Brain Res 2002;146(1):60–9.
[21] Mochizuki L, Duarte M, Amadio AC, Zatsiorsky VM, Latash ML. Changes in postural sway and its fractions in conditions of postural instability. J Appl Biomech 2006;22(1):51–60.
[22] Doumas M, Smolders C, Brunfaut E, Bouckaert F, Krampe RT. Dual task performance of working memory and postural control in major depressive disorder. Neuropsychology 2011;26(1):110–8.
[23] Duarte M, Freitas SMSF. Revision of posturography based on force plate for balance evaluation. Rev Bras Fisioter 2010;14:183–92.
[24] Duarte M, Freitas SMSF, Zatsiorsky V. Control of equilibrium in humans – sway over sway. In: Latash M, Danion F, editors. Motor control. Oxford: Oxford University Press; 2011. p. 219–42.
[25] Kirchner M, Schubert P, Schmidtbleicher D, Haas CT. Evaluation of the temporal structure of postural sway fluctuations based on a comprehensive set of analysis tools. Physica A 2012;391(20):4692–703.
[26] Maurer C, Peterka R. A new interpretation of spontaneous sway measures based on a simple model of human postural control. J Neurophysiol 2005;93(1):189–200.
[27] Ruhe A, Fejer R, Walker B. The test-retest reliability of centre of pressure measures in bipedal static task conditions – a systematic review of the literature. Gait Posture 2010;32(4):436–45.
[28] Winter D. Biomechanics and motor control of human movement. 4th ed. Hoboken, New Jersey: John Wiley & Sons; 2009.